Supporting information

Highly Stereoselective Bimetallic Complexes for Lactide and ε-Caprolactone Polymerization

Xuan Pang, Ranlong Duan, Xiang Li, Zhiqiang Sun, Han Zhang, Xianhong Wan and Xuesi Chen

Key Laboratory of Polymer Ecomaterials, Changchun Institute of Applied Chemistry, Chinese Academy of Sciences, Changchun 130022, China
Correspondence to: Xuesi Chen (E-mail: xschen@ciac.ac.cn)

Calculation of the entropy and enthalpy difference between homo-propagation and cross-propagation

In a first-order Markovian statistics, PLA derived from *rac*-lactide could exhibit up to five tetrad sequences (mmm, mmr, rmm, mrm, rmr) in relative ratios determined by the ability of initiators to control racemic [r-diad] and meso [m-diad] connectivity of the monomer units. According to first-order Markovian statistics, the probability for *meso* linkages could be determined as

$$P_m = k_m/(k_m + k_r) = k_{S/SS}/(k_{S/SS} + k_{S/RR}) = k_{R/RR}/(k_{R/SS} + k_{R/RR}) \quad (S1)$$

where $k_{S/SS}$ and $k_{R/RR}$ were the rate constants of homopropagation, $k_{S/RR}$ and $k_{R/SS}$ were the rate constants of cross propagation. If $k_{S/SS} > k_{S/RR}$ or $k_{R/RR} > k_{R/SS}$, the formation of isotactic sequences were favored, otherwise syndiotactic sequences were formed. The following equations could be deduced according to absolute reaction rate theory:

$$k_{S/SS} = k_{R/RR} = k_m = (KT/h)\exp[(\Delta S^{\neq}_{m}/R) - (\Delta H^{\neq}_{m}/RT)] \quad (S2)$$

$$k_{R/SS} = k_{S/RR} = k_r = (KT/h)\exp[(\Delta S^{\neq}_{m}/R) - (\Delta H^{\neq}_{m}/RT)] \quad (S3)$$

Further deduction of equation S4 could be obtained from equation S2 and equation S3:

$$P_m/(1 - P_m) = k_m/k_r = \exp[(\Delta S^{\neq}_{m} - \Delta S^{\neq}_{m})/R - (\Delta H^{\neq}_{m} - \Delta H^{\neq}_{m})/RT] \quad (S4)$$

where $(\Delta S^{\neq}_{m} - \Delta S^{\neq}_{m})$ was the entropy difference between homopropagation and cross propagation, and $(\Delta H^{\neq}_{m} - \Delta H^{\neq}_{m})$ was the enthalpy difference between homopropagation and cross propagation. To determine the values of $(\Delta S^{\neq}_{m} - \Delta S^{\neq}_{m})$ and $(\Delta H^{\neq}_{m} - \Delta H^{\neq}_{m})$, $\ln P_m/(1 - P_m)$ was plotted versus the 1/T (Figure S1). From this plot, the entropy difference $(\Delta S^{\neq}_{m} - \Delta S^{\neq}_{m})$ of –17.19 cal/K·mol and activation enthalpy difference $(\Delta H^{\neq}_{m} - \Delta H^{\neq}_{m})$ of –7.33 kcal/K·mol were obtained, which may explain the preference of isotactic stereosequence.

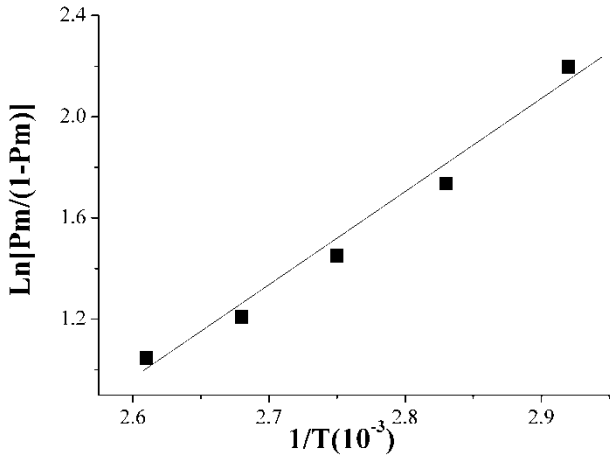

Figure S1 Relationship between polymerization temperature and stereochemistry of the resulting poly(rac-LA)s by using complex **3a**.

^{1}H and ^{13}C NMR spectra for all ligands and complexes

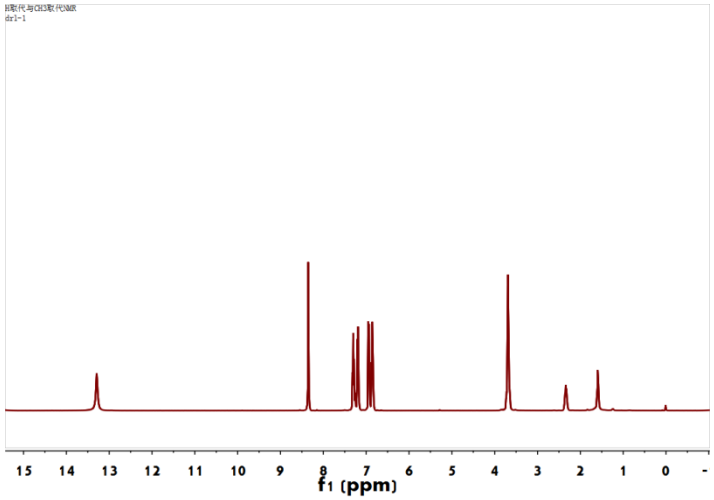

Figure S2 ^{1}H NMR spectra of ligand 1.

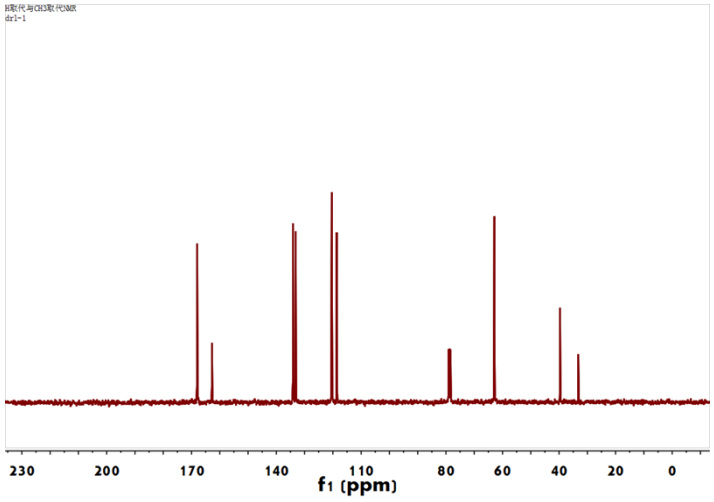

Figure S3 ^{13}C NMR spectra of ligand 1.

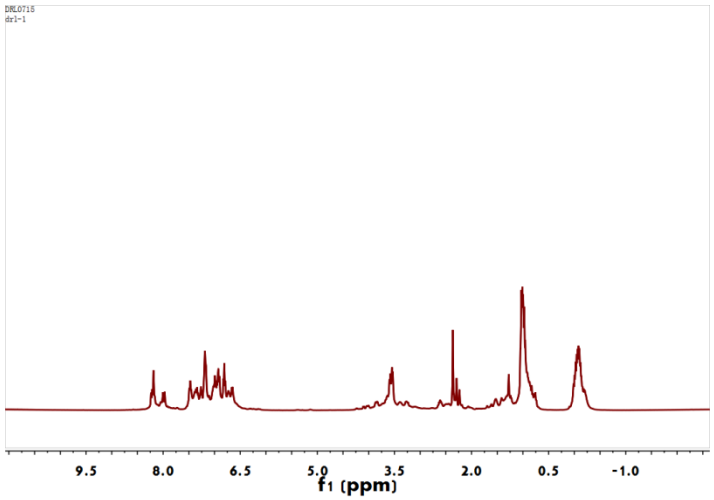

Figure S4 ^{1}H NMR spectra of 1a.

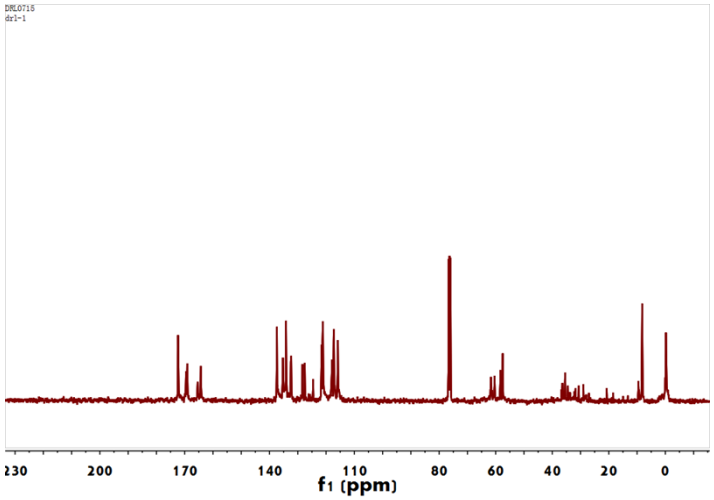

Figure S5 ^{13}C NMR spectra of 1a.

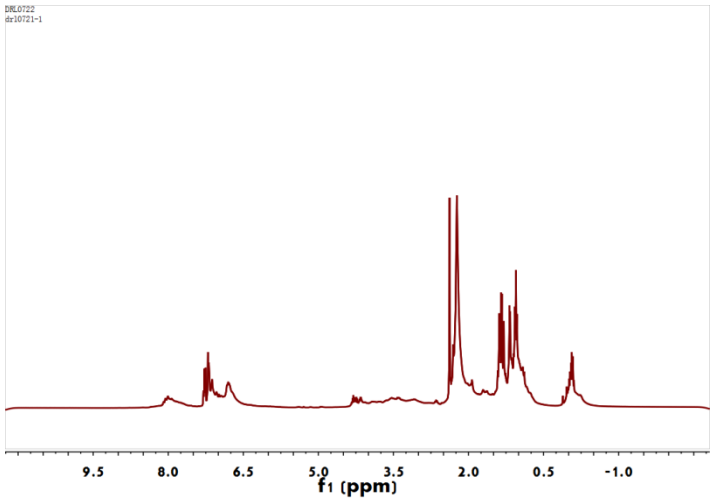

Figure S6 ^{1}H NMR spectra of 1b.

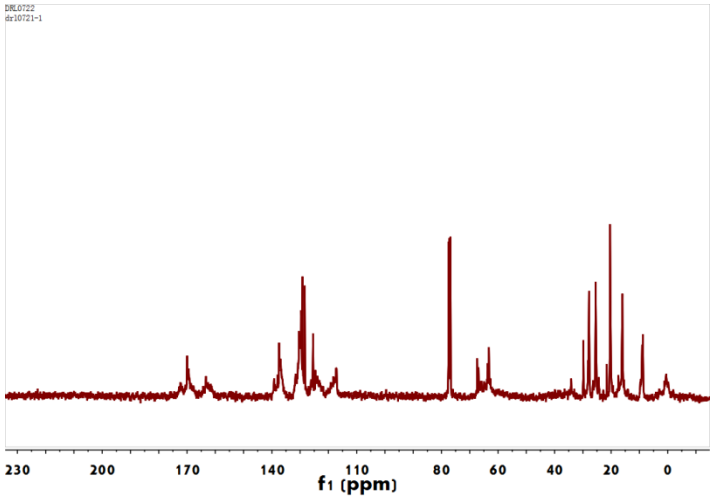

Figure S7 ^{13}C NMR spectra of 1b.

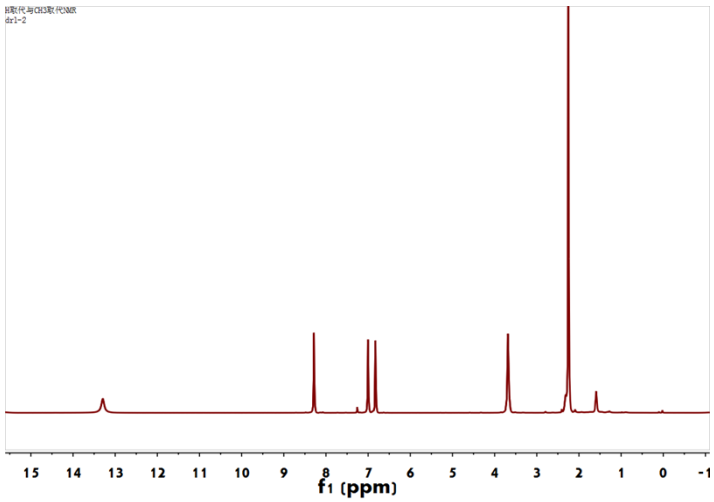

Figure S8 ^{1}H NMR spectra of ligand 2.

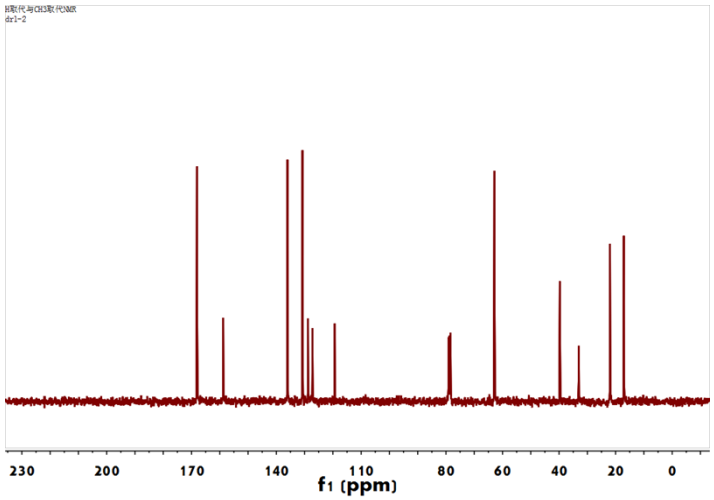

Figure S9 ^{13}C NMR spectra of ligand 2.

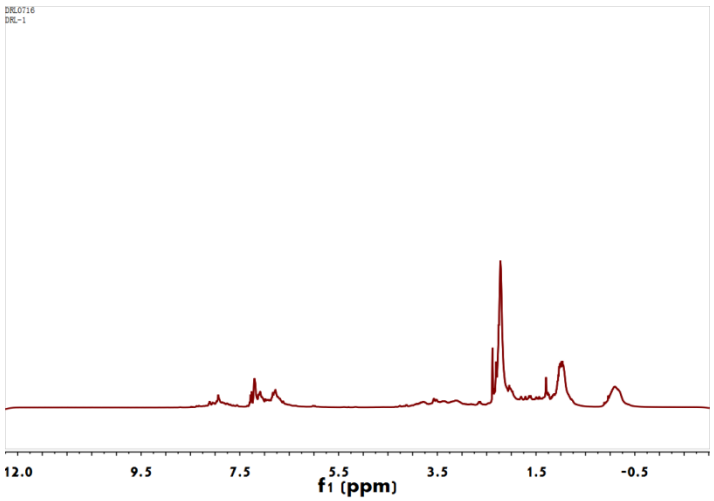

Figure S10 ^{1}H NMR spectra of 2a.

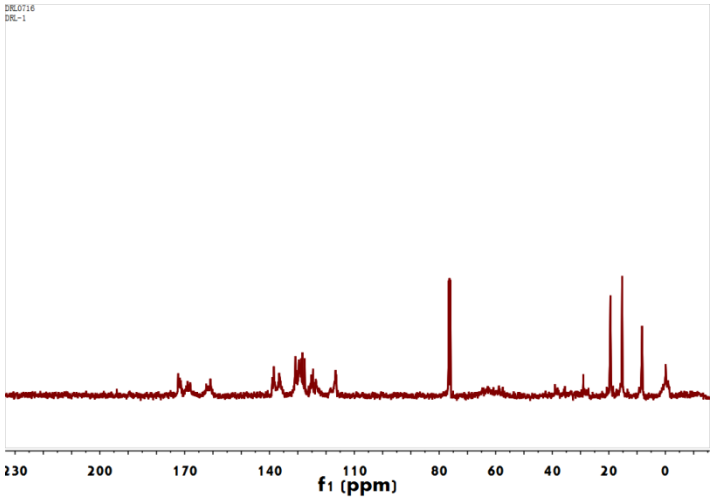

Figure S11 ^{13}C NMR spectra of 2a.

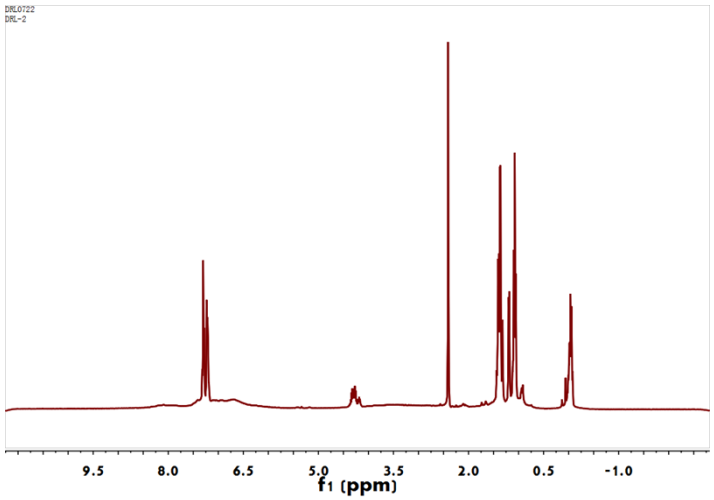

Figure S12 ^{1}H NMR spectra of 2b.

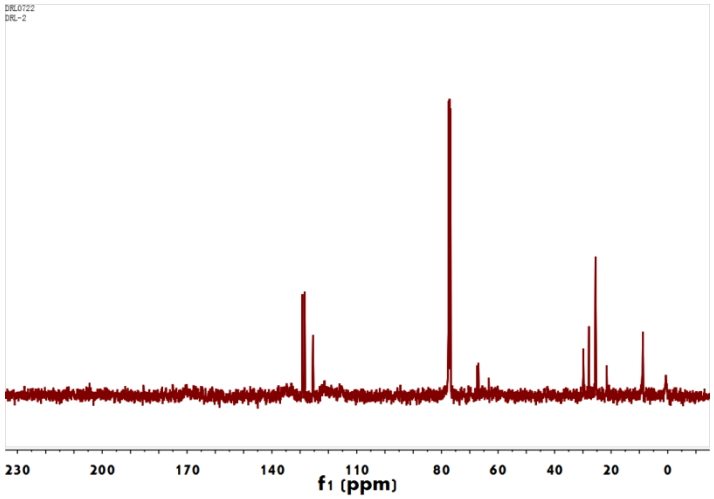

Figure S13 ^{13}C NMR spectra of 2b.

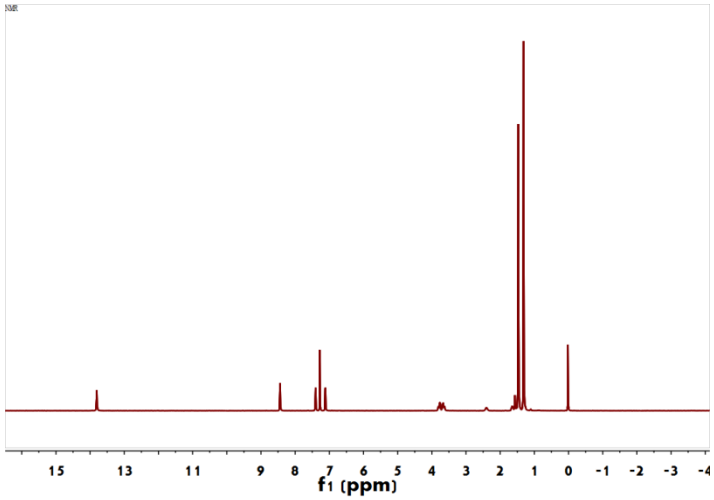

Figure S14 ^{1}H NMR spectra of ligand 3.

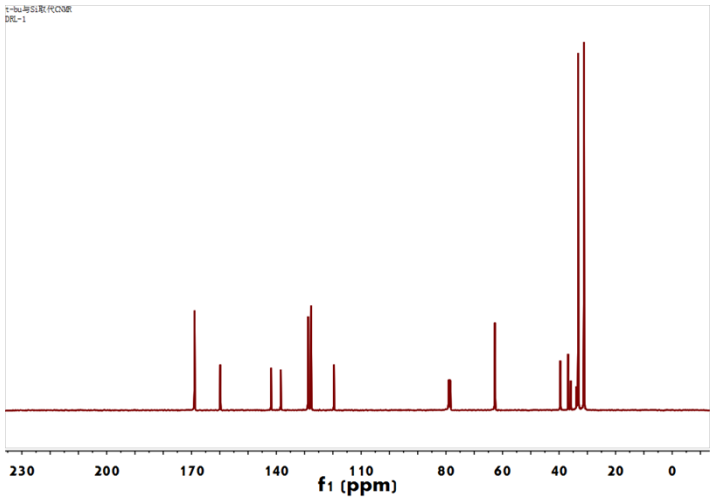

Figure S15 ^{13}C NMR spectra of ligand 3.

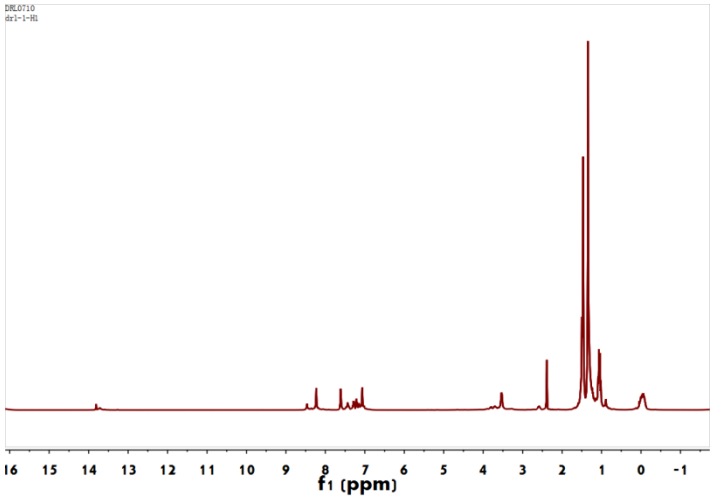

Figure S16 ^{1}H NMR spectra of 3a.

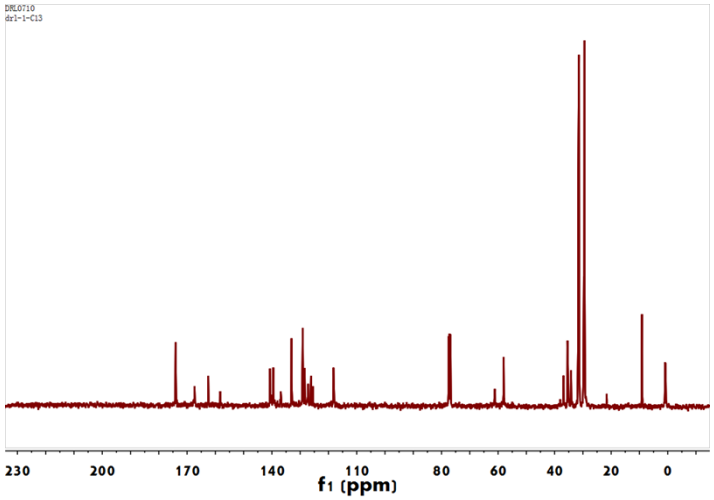

Figure S17 ^{13}C NMR spectra of 3a.

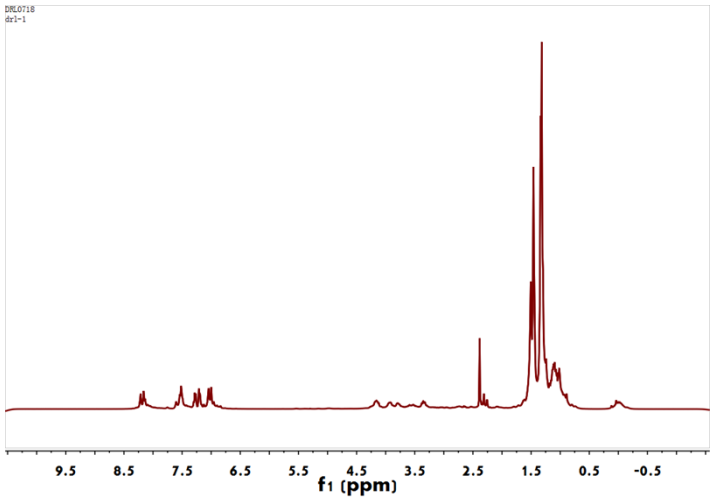

Figure S18 ^{1}H NMR spectra of 3b.

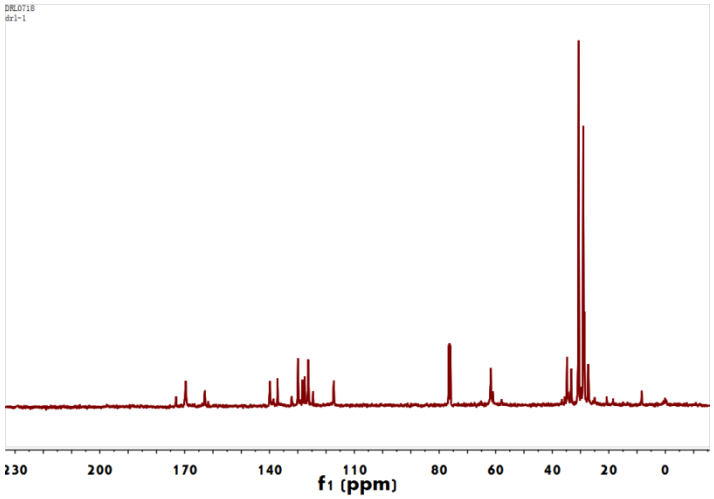

Figure S19 ^{13}C NMR spectra of 3b.

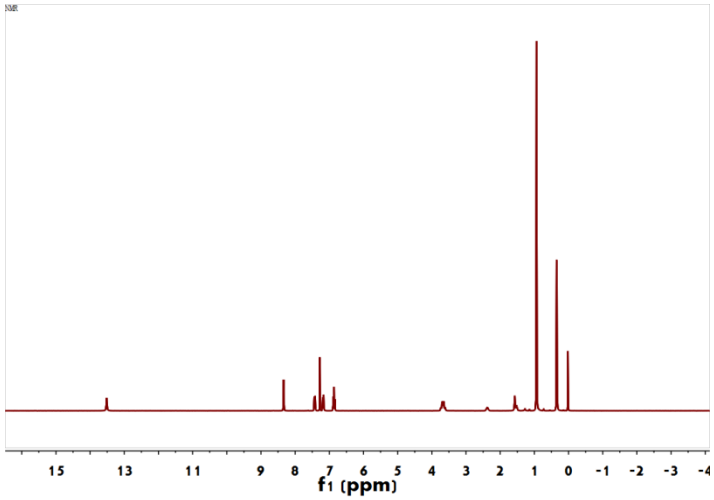

Figure S20 ^{1}H NMR spectra of ligand 4.

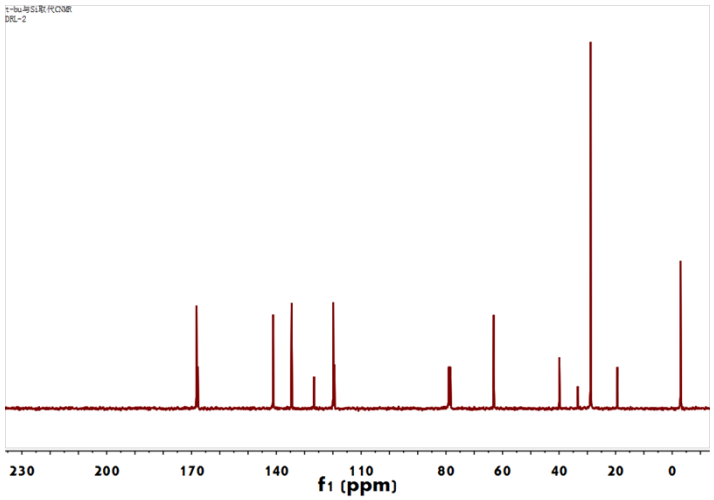

Figure S21 ^{13}C NMR spectra of ligand 4.

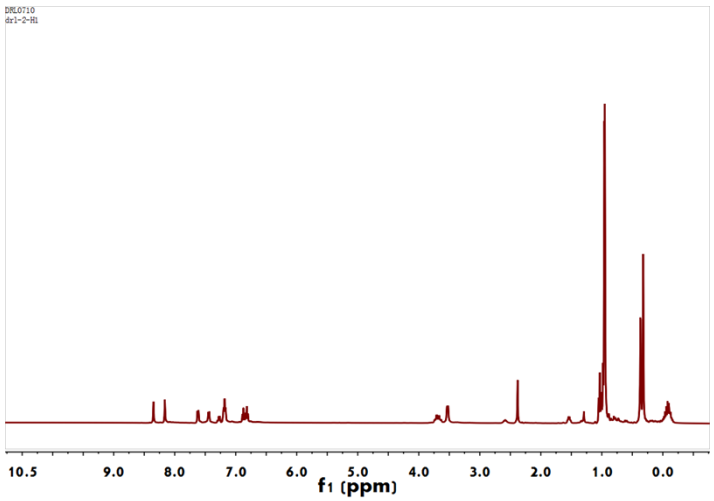

Figure S22 ^{1}H NMR spectra of 4a.

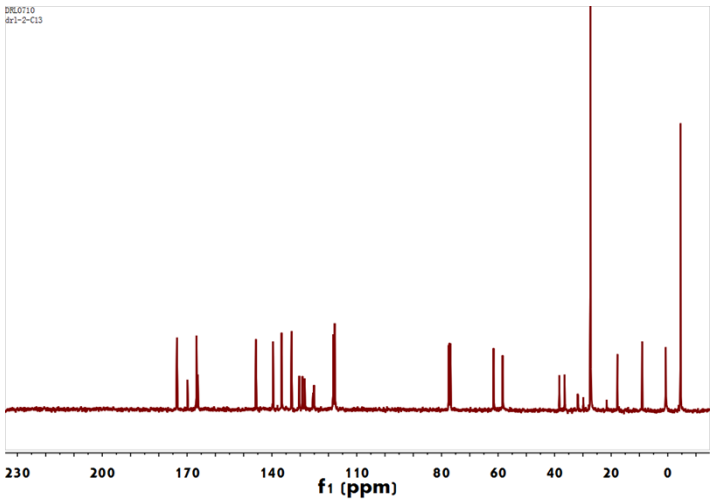

Figure S23 ^{13}C NMR spectra of 4a.

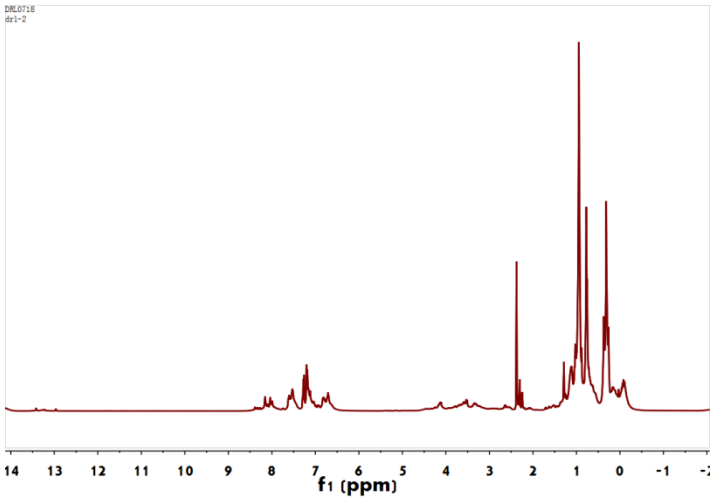

Figure S24 ^{1}H NMR spectra of 4b.

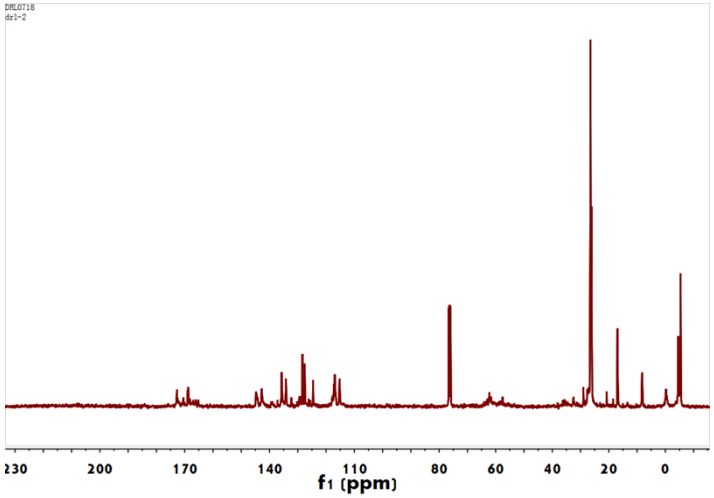

Figure S25 ^{13}C NMR spectra of 4b.

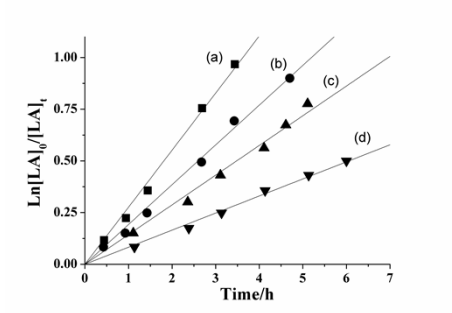

Figure S26 Kinetic plots of the *rac*-lactide conversion vs. the reaction time using complex **3a**: (a) $[M]_0/[cat]=100$; (b) $[M]_0/[cat]=150$; (c) $[M]_0/[cat]=200$; (d) $[M]_0/[cat]=300$.

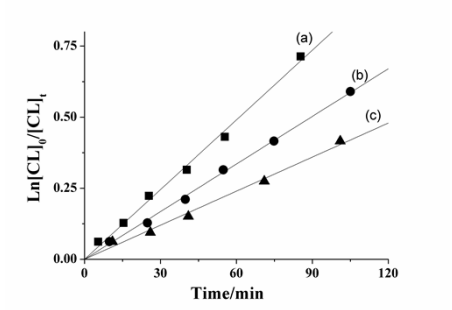

Figure S27 Kinetic plots of the ε-CL conversion vs. the reaction time using complex **3a**: (a) $[M]_0/[cat]=150$; (b) $[M]_0/[cat]=200$; (c) $[M]_0/[cat]=300$.

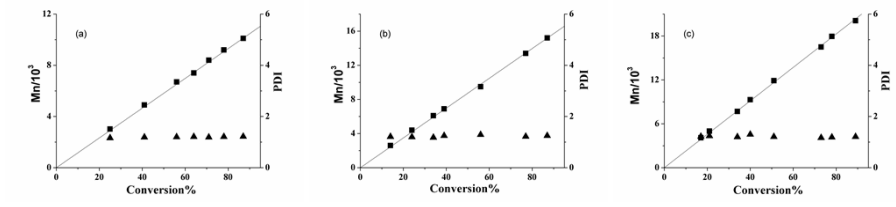

Figure S28 Plot of PCL Mn (■) and polydispersity (▲) as a function of ε-CL conversion using (a) complex **1a**, $[M]_0/[cat]=200$; (b) complex **3a**, $[M]_0/[cat]=300$; (c) complex **3a**, $[M]_0/[cat]=400$.